



# Distribution of bacterial single cell parameters and their estimation from turbidity detection times

Anna Jánosity<sup>a</sup>, Balázs Vajna<sup>b</sup>, Gabriella Kiskó<sup>a</sup>, József Baranyi<sup>c,\*</sup>

<sup>a</sup> Hungarian University of Agriculture and Life Sciences, Department of Food Microbiology, Hygiene and Safety, Budapest, Hungary

<sup>b</sup> Eötvös Loránd University, Department of Microbiology, Budapest, Hungary

<sup>c</sup> Institute of Nutrition, University of Debrecen, Hungary

## ARTICLE INFO

### Keywords:

Single cell kinetics  
Turbidity  
Single cell  
Lag time  
Physiological state

## ABSTRACT

The stochastic growth of homogeneous bacterial populations in the wells of a microtiter plate was studied as a function of the random initial cell number and their random individual lag times. These significantly affected the population growth in the well, while the maximum specific growth rate of the population was constant (or its variance was negligible) for each well.

We showed the advantages of the mathematical assumption that a transformation of the single cell lag time, called the single cell physiological state (or, more accurately, that of the sub-population generated by the single cell) follow the Beta distribution. Simulations demonstrated what patterns would such assumption generate for the distribution of the detection times observed in the wells. An estimation procedure was developed, based on the beta-assumption, that resulted in an explicit expression for the expected value of the single cell physiological state as a function of measured “time to detection” values using turbidity experiments. The method was illustrated using laboratory data with *Escherichia coli*, *Salmonella enterica* subsp. *enterica* strains. The results gave a basis to quantify the difference between the studied organisms in terms of their single-cell kinetics.

## 1. Introduction

The field of food microbiology has been typically featured with experiments performed at population levels when many cells collective behaviour is measured. However, at lower cell concentrations, the randomness of the individual cell responses has much greater influence on the collective growth than it does at higher concentrations. It is therefore of foremost importance to use stochastic modelling approaches to study bacterial growth in food matrices where pathogens usually occur at low concentrations (Koutsoumanis, 2008).

Automated turbidimeters are convenient tools to assess bacterial growth kinetics (Francois et al., 2005; Guilier and Augustin, 2006). A main disadvantage of this method is that it only detects turbidity when the cells are at high concentrations (typically higher than  $10^7$  cells/mL). Accordingly, when authors use turbidity measurements to describe single cell kinetics, the results are more about single-cell-generated subpopulations than about single cells. For example, the single cell lag time observed this way is in fact the traditionally (geometrically) defined lag time of the single-cell-generated subpopulation, which is different from the physiological single cell of the original ancestor cell

(Baranyi et al., 2009). The focus of this paper will also be the single cell lag time defined by the geometrical way, while assuming that the specific growth rate of the generated subpopulation is constant, or at least its variability is negligible compared to that caused by the single cell lag time interpreted in the way above.

The other random variable will be the number of initial cells in a well. Its expected value and variance can be estimated by means of the safe assumption that the initial cell number follows the Poisson distribution. In this case, the negative natural logarithm of the proportion of empty wells (in which no cells were inoculated) can be used to estimate the Poisson-parameter, which is the expected value of the initial number of cells per well. Strictly speaking, we should not claim that those wells for which no turbidity could be observed really did not receive cells at inoculation. It could have well happened that simply the growing cells did not reach the detection level during the observation time, either due to the very long lag time(s) of the initial cell(s), or because the cells did not divide at all but remained Viable but Non-culturable (VNC) cells.

We show an experimental protocol and an estimation procedure for some suitable parameters that can describe the distribution of single cell lag times. We apply the parameter estimates to quantify the difference between the studied organisms in terms of their single cell kinetics.

\* Corresponding author. Institute of Nutrition, University of Debrecen, H-4032, Debrecen, Böszörményi út 138, Hungary.

E-mail address: [baranyi.jozsef@med.unideb.hu](mailto:baranyi.jozsef@med.unideb.hu) (J. Baranyi).

<https://doi.org/10.1016/j.fm.2021.103972>

Received 31 August 2021; Received in revised form 15 December 2021; Accepted 17 December 2021

Available online 20 December 2021

0740-0020/© 2021 The Authors. Published by Elsevier Ltd. This is an open access article under the CC BY license (<http://creativecommons.org/licenses/by/4.0/>).

## Nomenclature

### Notation Meaning

$p, q, \alpha^*$	Parameters of the beta distribution, with $\alpha^*$ as an expected value
$\mu$	Maximum specific growth rate of the cell population; an environment- and species-determined constant
$w, W_0$	Total number of wells and the number of those wells that show no growth
$\rho, \rho^*$	Initial number of cells in a well, following the Poisson distribution, and its expected value, estimated by $\ln((w-2)/W_0)$
$\rho^+$	Initial number of positive cells (i.e. with at least one cell) in a well, following the positive Poisson distribution. Its expected value is $E(\rho^+) = \frac{e^{\rho}}{e^{\rho}-1}$
$OD_{det}, N_{det}$	OD level and the Number of cells in a well when the turbidity detection level is reached
$T_{det}(\rho)$	Time to reach the $N_{det}$ detection level for a cell population consisting of $\rho$ cells
$L_g(\rho)$	Lag time of a cell population consisting of $\rho$ cells
$\alpha(\rho), \alpha^*$	Physiological state of a cell population consisting of $\rho$ cells and its expected value (the same as for a single cell). $\alpha(\rho) = e^{-\mu \cdot L_g(\rho)}$
$S_\alpha$	$= \sum_{i=1}^{\rho} e^{-\mu \cdot L_g(i)}$ the sum of the physiological states for single cells in an initial population consisting of $\rho$ cells

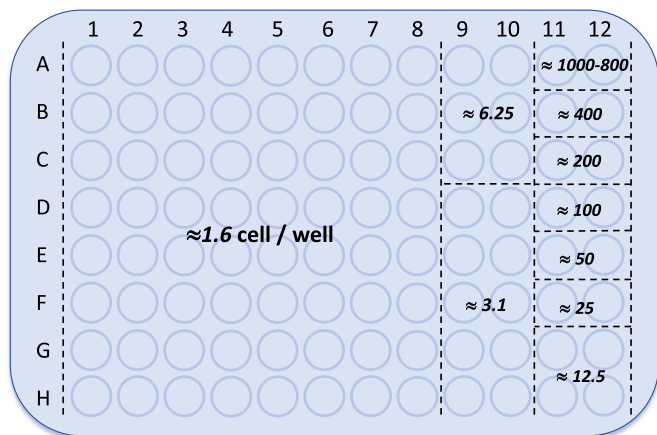


**Fig. 1.** Layout-1 of microtiter plates, prepared for turbidity measurements. The most replicates (64) were assigned to the lowest initial cell concentration (around 1.6 cell/well), then the number of replicate wells decreased with the inoculum level.

## 2. Material and methods

### 2.1. Organisms, inocula preparation and measuring their growth by a turbidimeter

The foodborne isolate *Escherichia coli* VF 3584 was provided by the Faculty of Veterinary Medicine, University of Ljubljana, Ljubljana, Slovenia. The Bacterial cultures *Escherichia coli* ATCC 25922, *Salmonella enterica* subsp. *enterica* ATCC 14028 and ATCC 13311 strains were obtained from the National Collection of Agricultural and Industrial Microorganisms, Budapest, Hungary. The cultures, which were derived from frozen stocks ( $-80^\circ\text{C}$ ), were cultivated twice on Tryptic Soy Agar plates (Basingstoke, Hampshire, UK), incubated at  $37^\circ\text{C}$  for 24 h before

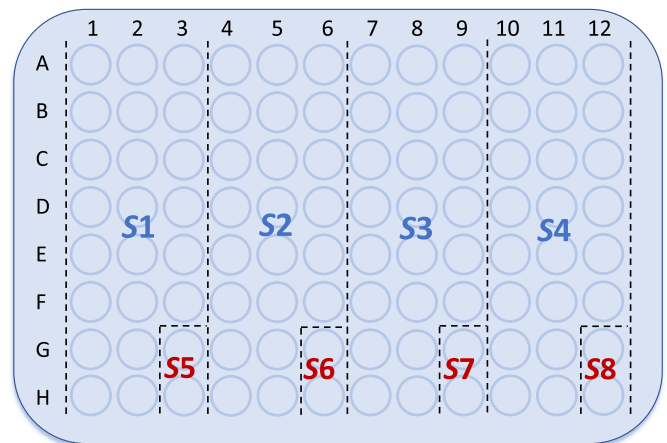


**Fig. 2.** Layout-2 of the microtiter plates. Plates were divided into 4 big blocks (S1–S4) of wells for the single cell level ( $<20$  cells per well) initial concentrations, and 4 small blocks (S5–S8) of wells for the population level (above ca.  $10^3$  cells per well) initial concentrations.

preparing overnight cultures. The overnight cultures were prepared as 4–5 bacterial colonies inoculated into 5 mL Mueller-Hinton II Broth (Biolab, Hungary) and grown at  $37^\circ\text{C}$  for 24 h.

Before the turbidity experiments, serial dilutions in Mueller-Hinton II Broth were applied to stationary phase cells. The aim was to obtain, via dilutions, ca. 1–3 cell/well for the lowest cell density on a microtiter plate. The final volume was 200  $\mu\text{L}$  per well. The initial concentration of inocula was set at  $OD_{600} = 0.1$  (Analytik Jena Specord 200 Plus Spectrophotometer). From this, we made four consecutive decimal dilutions, then 11–13 binary dilutions as needed to reach the desired cell concentration, to get ca. 1.6 cell/well, which was proven to be the optimum  $\rho^*$  for experiments to study single cells kinetics by Buss da Silva et al. (2019). Note, that the dilution rate was strain-dependent, this is why the above range for the number of binary dilutions; to be closer to the desired average number of initial cells in a well. The initial number was estimated by the proportion of those wells, which did not become turbid during the observation time.

Before each set of experiments, the concentrations of the binary diluted samples were also estimated by traditional plate counting. For Layout-1, we started the dilution series at ca.  $10^3$  cell/well, then ten consecutive binary dilutions were inoculated into the wells of a microtiter plate (Fig. 1). The design followed the idea of Baranyi and Pin (1999), expecting that the variance of the detection times decreases with inoculum level increasing.

Fig. 2 shows another layout with more obvious separation of single cell and population kinetics. Samples of the lowest four concentrations were inoculated into four blocks, each consisting of 22 wells of the microtiter plate, aiming at  $\rho^* = 1.6, 3.2, 6.4$  and  $12.8$  cells per well inocula (single cell level). At the same time, the specific growth rates were also measured starting from ca.  $10^7; 5 \cdot 10^6; 2.5 \cdot 10^6$  and  $1.25 \cdot 10^6$  cells per well (population level). This design was based on the idea that the maximum specific growth rate should be measured as accurately as possible, therefore at population level (S5–S8). On the other hand, the higher the inoculum, the higher its variance, so the number of replicate wells does not necessarily decrease with increasing inoculum level.

The optical density readings were produced right after the appropriate dilutions by an automated plate reader (Sunrise, Tecan Group Ltd., Switzerland). We recorded the time (called detection time,  $T_{det}$  in what follows) that was needed for the cultures to reach  $OD_{det} = 0.15$  (detection level) at 590 nm, when the number of cells in a well was  $N_{det}$  (detection level number of cells). The effect of individual cells on the variation of lag was investigated under optimum growth conditions at  $37^\circ\text{C}$  for 24 h. Readings were made in every 30 min, with 20 s of shaking time prior them. The distribution of  $T_{det}$  was considered a shifted version

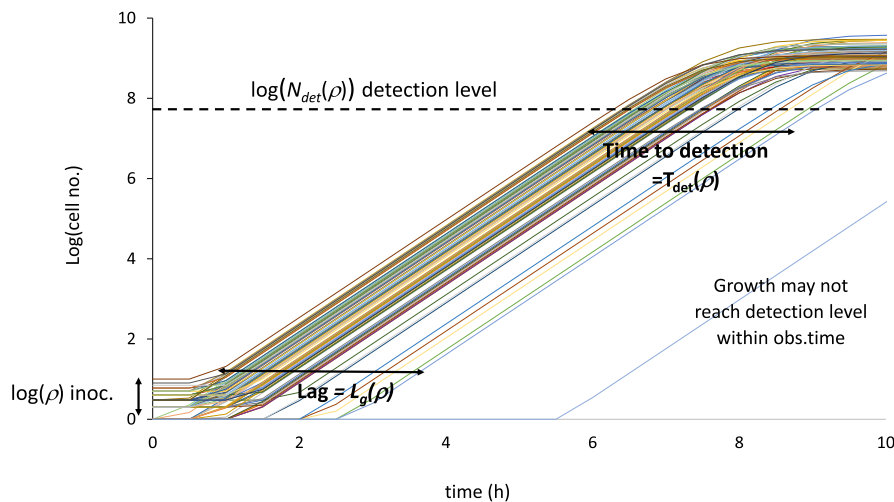


**Fig. 3.** Simulating the logarithm of cell numbers in the wells, assuming Poisson distributed initial cell numbers and beta-distributed single-cell physiological states. The design followed the one shown by Fig. 2; i.e. using 4 blocks of 22 wells, where the inoculum for the block of the lowest level consisted of 22 wells. The other  $\rho^*$  Poisson parameters followed the rule  $\rho_j^* = 2\rho_{j-1}^*$ , ( $j = 1, 2, 3$ ).  $N_{det}$  was set to  $10^{7.8}$  cell/well as suggested by plate count estimations for the  $OD_{det} = 0.15$  level.

of the distribution of lag times in the wells, as the maximum specific growth rate was assumed to be the same for all wells. The  $N_{det}$  of each strain were estimated by the traditional spread plate method as in George et al. (2015).

## 2.2. Inoculum and single cell lag time as stochastic variables

The number of initial cells in a well,  $\rho$ , is a Poisson-distributed random variable. Its expected value can be obtained (i) by an *a-priori* estimate,  $c^*$ , based on the original cell concentration, the consecutive dilutions, and the volume of a well; and (ii) by an *a-posteriori* estimate as in Buss da Silva et al. (2019), who showed that  $\rho^* = \ln((w-2)/W_0)$  is an efficient estimation for the expected number of initial cells in a well, where  $w$  is the total,  $W_0$  is the empty number of wells. The  $\rho^*/c^*$  ratio can be used to estimate the probability of growth for single cells, but only for values significantly less than 1 (George et al., 2015).

The initial cells produce an exponentially growing subpopulation in the well, showing, after a lag phase, a linear trend on the log-scale (Fig. 3). The lag time of a single-cell-generated growth curve is traditionally defined as the time where extension of this linear phase crosses the inoculum level. This geometrically interpreted lag time will be denoted by  $L_g(\rho)$ , indicating that it depends on the Poissonian  $\rho$  initial cell number. The distribution of  $L_g(\rho)$  is a convolution of  $\rho$  and the  $L_g(1)$  single cell lag times. This latter variable was assumed by Métris et al. (2006) to follow the Gamma distribution.

Because the specific growth rate is constant so, as long as the  $T_{det}(\rho)$  detection time is in the exponential phase, it is just a shifted version of  $L_g(\rho)$ . A central question of this paper is whether there is a simple way to draw conclusions, from the  $T_{det}(\rho)$  measured values, for the distribution of the  $L_g(1)$  single cell lag time.

## 2.3. Physiological-state-parameter and its distribution for individual cells

Métris et al. (2006) and D'Arrigo et al. (2006) used the gamma distribution with shape parameter 2 (as if  $L_g(1)$  was the sum of two exponentially distributed times) to model the single cell lag time. The novelty of our paper is to introduce a more advantageous approach.

Baranyi and Pin (1999) demonstrated the usefulness of the quantity "physiological state" for the initial cell population consisting of  $N$  cells. Its definition is:

$$\alpha(N) = e^{-\mu L_g(N)}$$

with the interpretation as follows: if an  $\alpha$  proportion of the  $N$  initial cells had grown immediately after inoculation, without lag, while the rest hadn't grown at all, then their growth curve would have arrived at the same exponential phase trajectory that the observed full population exhibits. This interpretation lends itself to assuming the Beta distribution for the  $\alpha(1)$  single-cell physiological state, as this distribution is primarily used to describe random proportions. In our case, the lag can be calculated by inverting the above transformation:  $L_g(1) = -\ln(\alpha(1))/\mu$ . It is easy to see that the lag obtained this way follows a distribution that is different from the gamma distribution; though, for a wide range of parameters, very close to it.

The idea looks like just another option, among the possible mathematical assumptions; however, it has certain advantages. Namely, as the physiological state of the population was proven to be the average of the physiological states of its single cells, this property can be utilized to simplify the calculations, as the mean physiological state can be directly estimated from the detection times (see Appendix), generating the following estimation procedure:

- Establish the  $\mu$  exponential growth rate (measured on the natural log scale) via independent optical density readings at population level (greater than say  $10^3$  cell/ml inoculum - Figs. 1 and 2.)
- Run turbidity experiments as above, with different  $\rho^*$  expected cell/well inocula, aiming at its lowest level to be between 1 and 3. For every  $\rho^*$ , calculate

$$h_0(\rho^*) = -\ln\left(\frac{N_{det}}{\rho^*} \cdot \text{average}\left(e^{-\mu T_{det}(\rho_i)}\right)\right)$$

where the  $i$  indices belong to the wells with the  $\rho^* > 0$  Poisson parameter. The average of these  $h_0(\rho^*)$  values, when  $\rho^*$  is small (ca.  $\rho^* \leq 10$ ; see Fig. 2), is an estimation for  $h_0^* = -\ln(\alpha^*)$

- Fix the sum of the two parameters ( $p, q$ ) of the beta distribution at the value of  $S_{pq} = 5$  as mentioned in the Appendix. This is equivalent to fixing the shape-parameter 2 of the Gamma distribution for the single cell lag time. Then  $p = S_{pq} \cdot \alpha^*$  and  $q = 1-p$  will complete the procedure.

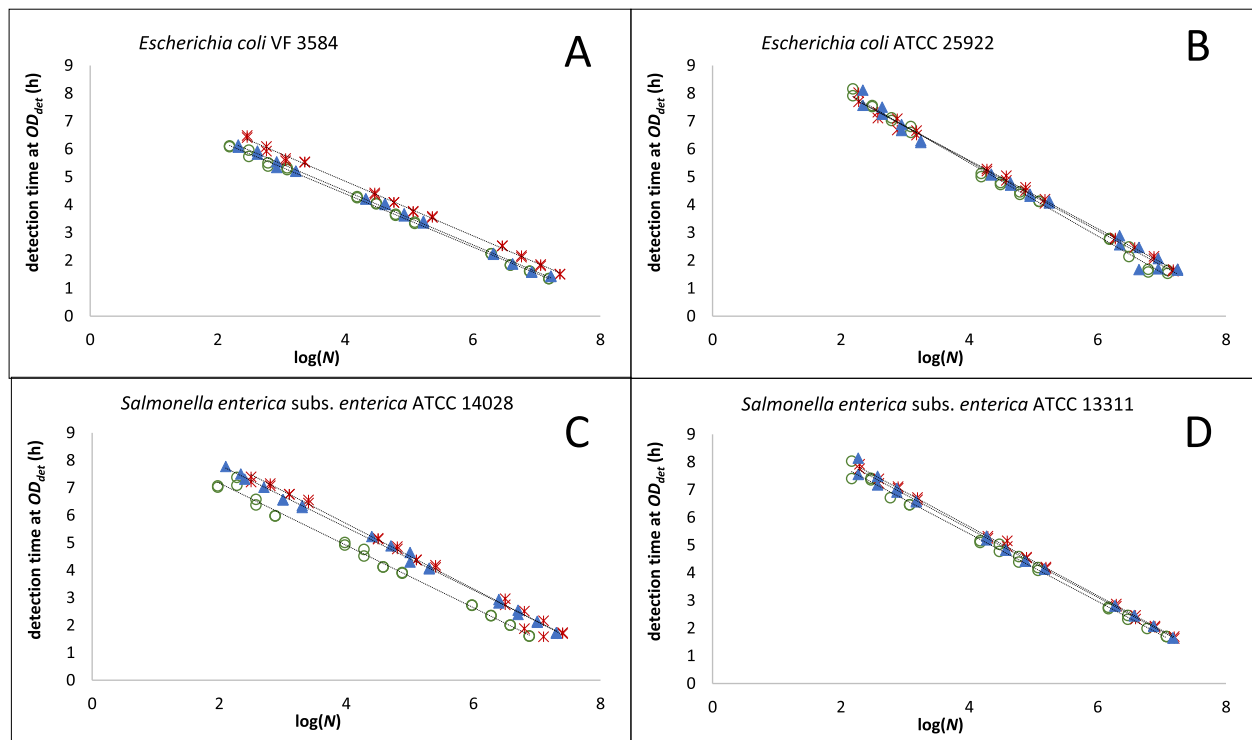


**Fig. 4.** Detection times v.  $\log(N)$  plots, where  $N \approx 10^3$ ,  $10^5$  and  $10^7$  cells per well. The plots demonstrate how well OD readings can be used to obtain robust estimates for the maximum specific growth rate via three independent replicates. Capital letters are to distinguish between the microorganisms (see also Table 2).

**Table 1**

Cell numbers of each strain per well at the detection level ( $OD_{det} = 0.15$  at 590 nm), measured by spread plate technique. The highlighted concentrations are average values of three independent replicates.

Strains in Mueller-Hinton II Broth	$N_{det}$ ( $OD_{det} = 0.15$ ) (cell/well)
<i>Escherichia coli</i> VF 3584	7.54·10 <sup>7</sup>
<i>Escherichia coli</i> ATCC 25922	6.96·10 <sup>7</sup>
<i>Salmonella enterica</i> subsp. <i>enterica</i> ATCC 14028	7.42·10 <sup>7</sup>
<i>Salmonella enterica</i> subsp. <i>enterica</i> ATCC 13311	8.98·10 <sup>7</sup>

### 3. Results

#### 3.1. Model simulation

Fig. 3 was prepared with  $\mu = 2.8 \text{ h}^{-1}$  and  $\alpha^* = 0.1$ . This value for the mean physiological state is typical for *E. coli*, in optimal conditions, assuming standard inoculation procedure (see [www.ComBase.cc](http://www.ComBase.cc)). The maximum population density was set to  $10^9$  cell/ml, with 0.5  $\log_{10}$  unit standard deviation, as this is also typical for batch cultures of *E. coli*. The  $S_{pq} = p + q$  sum was set as  $S_{pq} = 5$ , but also tested for values from 2 to 8 (see the Appendix), only to see that it did not significantly affect the simulated growth patterns.

As the specific growth rate significantly affects the estimation of the mean physiological state, when validating the estimation procedure by simulations, we fixed the  $\mu$  parameter at the value used in the simulation. Laboratory results (see Fig. 4) demonstrates that  $\mu = \text{constant}$  is a reasonable assumption. After repeating the simulation 100 times, with  $\alpha^* = 0.1$ , the developed estimation procedure proved to be ca. 5% accurate for  $h_0^* = -\ln \alpha^*$  (the average of the 100 trials was 2.28, with a standard deviation of 0.1 and with a close-to-gamma distribution; recall that the real value was  $-\ln(0.1) = 2.3$ ). This means that the mean physiological state was estimated at better than 20% accuracy. We also performed 100 simulations with Layout-1 (Fig. 1) and the accuracy of the mean physiological state estimate was similar.

**Table 2**

Specific growth rates and doubling times for the studied strains as calculated from Fig. 4.

	Specific growth rate $\mu$ ( $\text{h}^{-1}$ )	Doubling time $60 \cdot \ln(2) / \mu$ (min)
<i>Escherichia coli</i> VF 3584	$2.40 \pm 0.015$	17.33
<i>Escherichia coli</i> ATCC 25922	$1.82 \pm 0.011$	22.85
<i>Salmonella enterica</i> subsp. <i>enterica</i> ATCC 14028	$2.04 \pm 0.023$	20.38
<i>Salmonella enterica</i> subsp. <i>enterica</i> ATCC 13311	$1.87 \pm 0.010$	22.34

#### 3.2. Experimental results

The estimation procedure was tested on laboratory data using four organisms. To establish the maximum specific growth rate for each, we applied the binary dilution method to population level initial cell numbers *per well* (i.e. between  $10^3$  and  $10^7$ ). The experiments with low inocula, on the other hand, provided estimates for the  $\alpha^*$  mean physiological state for individual cells.

Table 1 shows various strains' cell numbers measured at  $OD_{det}$  level in Mueller-Hinton II Broth by the traditional plate count method. Note that, in the paper of George et al. (2015), the authors measured lower concentrations ( $N_{det} = 10^{7.2}$  cells at 0.15 OD). The difference could be explained by the uncertainty in the initial absorbance of the applied broths.

On Fig. 4, the detection times of consecutive diluted samples are plotted against  $\log(N)$  where  $N = \rho^*$  is the expected initial cell number in a well, the highest being around  $N = 10^7$  cell/well. The  $\mu$  specific growth rates, i.e. growth rate in terms of  $\ln(\text{cell.no})/\text{h}$ , was calculated as  $\mu = \ln(10)/a$ , where  $a$  is the slope of the fitted line. Table 2 shows the specific growth rates calculated from the data of Fig. 4. As can be expected from the plots, the replicates, denoted by different symbols, generate practically identical growth rates for the strains.

**Table 3**

Model parameter estimates obtained mainly via Layout-1, partly via Layout-2. The specific growth rate was estimated via population-level inocula. The  $h_0$  estimates were generated by single cell level inocula.

ORGANISM	Initial cell numbers per well, $c^*$ , estimated from plate counts and dilution factors	Initial cell numbers per well, $\rho^*$ , estimated from proportion of empty wells	$(h_0)_{\text{Estim}}$	$(\alpha^*)_{\text{Estim}}$
<i>Escherichia coli</i> VF 3584	1.99	4.13	2.6	0.074
	1.54	1.93	2.7	0.067
	1.71	1.90	1.8	0.165
	0.91	1.64	2.3	0.1
<i>Escherichia coli</i> ATCC 25922	4.19	3.43	1.1	0.333
	2.23	1.29	2.1	0.122
	0.63	1.05	3.3	0.037
<i>Salmonella enterica</i> subsp. <i>enterica</i> ATCC 14028	2.49	3.03	2.08	0.125
	1.51	2.33	1.89	0.151
	1.87	1.61	2.21	0.11
	0.65	0.66	1.14	0.32
<i>Salmonella enterica</i> subsp. <i>enterica</i> ATCC 13311	1.81	2.05	2.34	0.096
	1.67	1.29	2.01	0.134
	0.69	0.43	0.70	0.497

<sup>a</sup> Numbers are the log values of the applied dilution factors, from a cell concentration measured at  $OD=0.1$  considered as the 0 dilution.

<sup>b</sup> Gray highlighted rows represent data obtained according to the Layout-2; see Fig. 2.

A challenge we faced was to obtain ca. 1–3 initial cells per well concentration after the last binary dilution, as suggested by Buss da Silva et al. (2019). Table 3 contains the estimations for the initial cell/well numbers obtained via (1) combination of plate counts and dilutions ( $c^*$ ) and (2) by means of the proportion of empty wells ( $\rho^*$ ). Different rows

represent independent measurements. The first column,  $c^*$ , shows the estimated lowest cell number per well obtained via the first method. The starting point was the cell concentration obtained at  $OD_{600} = 0.1$  (0 dilution). First, 4 decimal, then  $11 \pm 2$  binary dilutions were applied to reach the lowest cell number. The second column,  $\rho^*$ , shows this inoculum level calculated by means of the proportion of empty wells. No significant difference was found between the two methods ( $p = 0.97$ ).

In the case of *Escherichia coli* VF 3584, after a concentration decrease of  $\log(\text{conc}) = 7.31$  (obtained after the eleventh binary dilution), we had three replicates  $\rho^* = 1.93$ ; 1.90 and 1.64, which means that setting the initial cell number is well reproducible. This is also supported by the fact that, at twice as high concentration ( $\log(\text{conc}) = 7.01$  decrease from the original one), we did measure about double as many cells ( $\rho^* = 4.13$ ).

The last column of Table 3 shows the respective estimates of  $h_0$ , from which  $\alpha^* = \exp(-h_0)$  is the mean single cell physiological state.

According to Buss da Silva et al. (2019), the relative error when estimating the initial number of cells in a well is ca. 20%, in the  $1 < \rho^* < 4$  interval. The accuracy level is the same for  $h_0$  so it's not surprising that the replicate experiments does not produce the same parameters. However, this inherent variability was not enhanced by the noise in the laboratory data.

Remember that  $\alpha$  can be conceived as a per cent measure how much ready the cells are for their new growth environment, while  $h_0 = \mu \cdot \lambda$  is a quantification of the work-to-be-done during the  $\lambda$  lag time. The average of the  $h_0$ -estimates (2.7) for *E. coli* in Table 2 shows that this organism was generally less prepared for the growth environment than *S. enterica*, for which the average of  $h_0$  was 1.7. This is also illustrated by Fig. 5C, on the scale of the physiological state, though the difference is not 95%-significant because of the relatively big variance of the replicate estimates.

Fig. 5A and B shows that, at low level of  $\rho^*$ , high variabilities can be observed in the detection time measurements. This is because both the initial cell number in a well, and the single cell lag times were random.

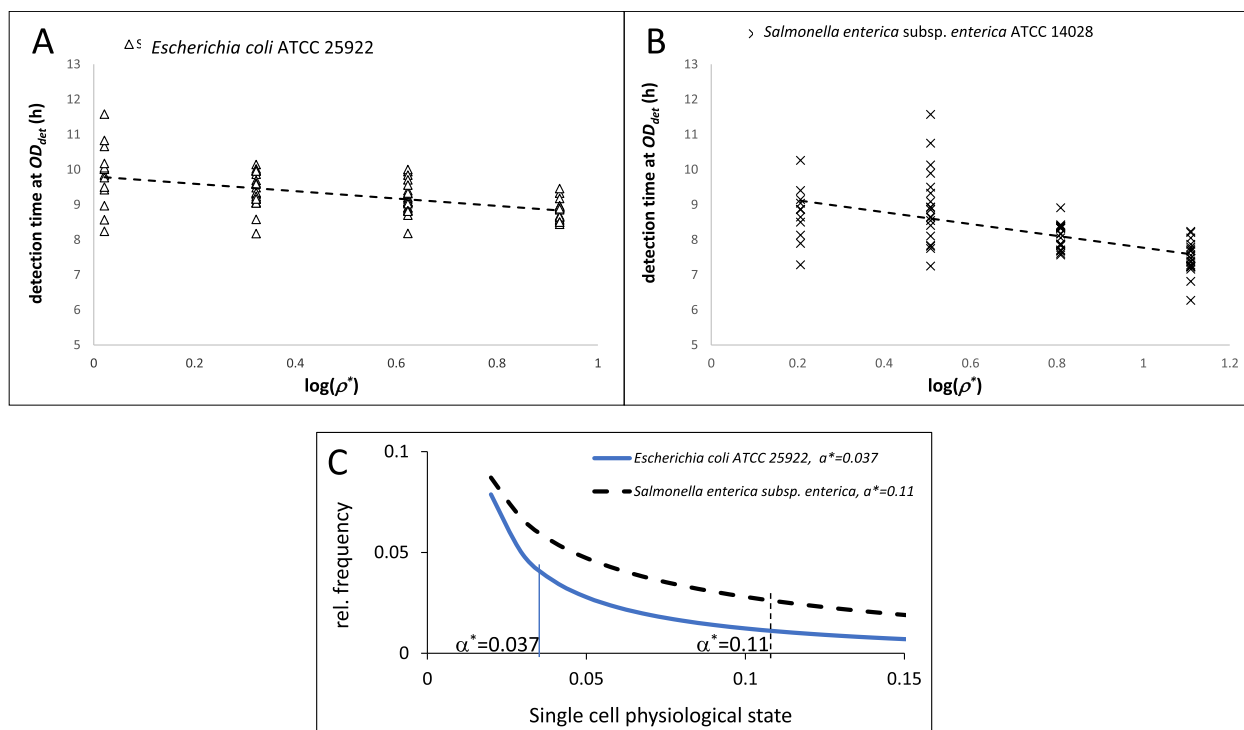


**Fig. 5.** Detection times generated by single cell level inocula for (A): *E. coli* ATCC 25922 and (B): *Salmonella enterica* subsp. *enterica* ATCC 14028. The lowest expected initial cell numbers per well were  $\rho^* = 1.05$  and  $\rho^* = 1.61$ . Detection times were measured in 22 wells according to Layout-2 (see Fig. 2.). (C): The two respective probability density functions for the single cell physiological state (broken line: *E. coli*; continuous line: *Salmonella enterica* subsp. *enterica*), generated by our estimation procedure.

We found that, below *ca.* 20 cells *per* well concentration, the variance of the  $T_{det}$  detection times of the *Salmonella* enterica strains was generally higher than that of the *E. coli* strains. This, could have well been due to the difference in the specific growth rates, but our method made it possible to confirm the difference at single cell level, too, by the distribution of the respective individual physiological states (Fig. 5C).

#### 4. Discussion

Buss da Silva et al. (2019) proved that, to assess single cell lag times, it is not necessary to aim at single cell inoculation in a well, when OD detection times are the only available measurements, but the properties of the Poisson distribution can be utilized for an efficient estimation procedure. Those authors found that if *ca.* 20–30% of the wells remain empty, i.e. after diluting the samples to *ca.* 1.6 cell/well level, then the accuracy of the Poisson parameter is at its optimum. We demonstrated that this is feasible to achieve in the laboratory, at reasonable accuracy. This played a vital role to measure single cell kinetics via turbidity measurements.

The present paper went one step further. When the Gamma-distribution was assumed for the distribution of single cell lag time (Métris et al., 2006; George et al., 2015), then the estimation procedure for the distribution parameters required a non-linear optimisation. We have shown here that the beta-distribution for the single cell physiological state is equally fitting, while the parameter estimation is reduced to an explicit formula, by which the mean physiological state can be directly calculated from the  $T_{det}(\rho)$  measured detection times, even though the initial number of cells in a well,  $\rho$ , is also random. Fixing the shape-parameter of the Gamma distribution at 2 proved (by simulation) to be equivalent to fixing the sum of the two (shape-) parameters of the Beta-distribution:  $p+q = 5$ . The obtained parameters can be used to characterize the readiness of the cells to the new environment, this way to quantify the difference between two organisms in terms of their adaptation ability (Fig. 5).

As for the experimental design, it is reasonable to think that the more initial cells are in a well, the fewer replicate wells are enough for stable variance. This was utilized by Layout-1, following the design of Baranyi and Pin (1999). However, this reasoning becomes invalid if the factor

between the two initial numbers is random, as in our case. Therefore, other practical considerations have become more important than stabilizing the variance; this led us to suggest Layout-2.

We saw that the average initial cell number *per* well ( $\rho^*$ ) can be compared with the respective estimates obtained by the dilution method ( $c^*$ ). The deviation between them is partly because, even if cells get in the well, they may not grow. Theoretically, the  $\rho^*/c^*$  ratio could be used to estimate the probability of growth at single cell level. However, strictly speaking, this ratio is the probability of the following event: either no cell has arrived in the well or the lineage of initial cells did not reach the detection level. Besides as both variables are random, with relatively large variance, it is rather difficult to estimate the error in their ratio, especially if that is close to zero or one.

The lower the initial cell concentration the more influence it has on the overall growth kinetics of the growing bacterial population due to the variability of single cell lag times. At very low initial cell numbers, under optimum growth conditions, the lag time variability of *Salmonella enterica* was higher than that of *E. coli*. This suggests that, under sub-optimal conditions, the difference between these time stretches would be even more significant. Quantification of this variability may have significance in the assessment of how long a specific food item can be stored while remaining safe. Our stochastic modelling technique and measurements with appropriate replicates at low initial cell numbers can help such assessments.

#### Declaration of competing interest

The authors declare that they have no known competing financial interests or personal relationships that could have appeared to influence the work reported in this paper.

#### Acknowledgment

The authors acknowledge the Doctoral School of Food Science of Hungarian University of Agriculture and Life Sciences for supporting this research. The project was funded by the New National Excellence Program of the Ministry of Innovation and Technology and by a National Research, Development and Innovation Award.

#### Appendix

The beta distribution is frequently used to model random proportions between 0 and 1. Its formula is typically written up with two shape-parameters,  $p$  and  $q$ , from which its expected value is.

$$E(\alpha(1)) = p/(p + q) = \alpha^*$$

while its variance is

$$\text{Var}(\alpha(1)) = \frac{p}{p+q} \cdot \frac{q}{p+q} \cdot \frac{1}{p+q+1}$$

As our focus is the  $\alpha^*$  expected value of  $\alpha(1)$ , we use the  $(\alpha^*, q)$  parameterisation, so  $p = q \cdot \alpha^*/(1-\alpha^*)$  and

$$\text{Var}(\alpha(1)) = \frac{\alpha^* \cdot (1 - \alpha^*)^2}{q + 1 - \alpha^*} \quad (\text{A1})$$

Based on the idea of Métris et al. (2006), let the sum of the physiological states of positive (non-empty) wells

$$S_\alpha = \sum_{i=1}^{\rho} \alpha_i(1)$$

where  $i$  refers to the single cells in a well. This is a Poissonian sum, i.e. the number of terms, denoted by  $\rho^+$  below, is random, following the positive Poisson distribution (as  $i = 0$  is excluded from  $S_\alpha$ ). Its expected value and variance are:

$$E(\rho^+) = \alpha^* \cdot \rho^* \cdot \frac{e^{\rho^*}}{e^{\rho^*} - 1} \quad (\text{A2})$$

$$\text{Var}(\rho^+) = E(\rho^+)(1 + \rho^* - E(\rho^+)) \quad (\text{A3})$$

Recall that the physiological state of the cell population in a well is the average of the individual physiological states (Baranyi and Pin, 1999). Due to simple geometry,

$$S_{\alpha} = \rho \cdot \alpha(\rho) = N_{det} e^{-\mu T_{det}(\rho)} \quad (\text{A4})$$

From the properties of the Poissonian sum of random variables:

$$\mathbf{E}(S_{\alpha}) = \alpha^* \cdot \mathbf{E}(\rho^+) = \alpha^* \cdot \rho^* \cdot \frac{e^{\rho^*}}{e^{\rho^*} - 1} \quad (\text{A5})$$

$$\text{Var}(S_{\alpha}) = \text{Var}(\rho^+) \cdot (\alpha^*)^2 + E(\rho^+) \cdot \text{Var}(\alpha(\mathbf{1})) \quad (\text{A6})$$

As  $\rho^*$  and  $N_{det}$  are estimated from the proportion of empty wells and from plate counting, respectively, so  $\alpha^*$  can be estimated from (A4)-(A5).

To estimate  $q$ , the sample variance for  $\text{Var}(S_{\alpha})$  could be used in (A6), giving an implicit equation for  $q$ . However, as this parameter defines the shape of the Beta distribution, it is more practical to recall that the  $L_g(1) = -\ln(\alpha(1))/\mu$ . Numerical experience shows that, at our range of parameters, the logarithm of a Beta-distributed random variable can be well approximated by Gamma-distribution. Its shape parameter 2 (see Métris et al., 2006), is about equivalent to  $2 < p+q < 8$ . Fixing this at  $S_{pq} = p+q = 5$  is sufficient for practical applications considering the range of other data and parameters.

## References

- Baranyi, J., Pin, C., 1999. Estimating bacterial growth parameters by means of detection times. *Appl. Environ. Microbiol.* 65, 732–736. <https://doi.org/10.1128/AEM.65.2.732-736.1999>.
- Baranyi, J., George, S.M., Kutalik, Z., 2009. Parameter estimation for the distribution of single cell lag times. *J. Theor. Biol.* 259, 24–30. <https://doi.org/10.1016/j.jtbi.2009.03.023>.
- Buss da Silva, N., Carciofi, B.A.M., Ellouze, M., Baranyi, J., 2019. Optimization of turbidity experiments to estimate the probability of growth for individual bacterial cells. *Food Microbiol.* 83, 109–112. <https://doi.org/10.1016/j.fm.2019.05.003>.
- D'Arrigo, M., García de Fernando, G.D., Velasco de Diego, R., Ordóñez, J.A., George, S. M., Pin, C., 2006. Indirect measurement of the lag time distribution of single cells of *Listeria innocua* in food. *Appl. Environ. Microbiol.* 72 (4), 2533–2538. <https://doi.org/10.1128/AEM.72.4.2533-2538.2006>.
- Francois, K., Devlieghere, F., Smet, K., Standaert, A.R., Geeraerd, A.H., Van Impe, J.F., Debevere, J., 2005. Modelling the individual cell lag phase: effect of temperature and pH on the individual cell lag distribution of *Listeria monocytogenes*. *Int. J. Food Microbiol.* 100, 41–53. <https://doi.org/10.1016/j.ijfoodmicro.2004.10.032>.
- George, S.M., Métris, A., Baranyi, J., 2015. Integrated kinetic and probabilistic modelling of the growth potential of bacterial populations. *Appl. Environ. Microbiol.* 81 (9), 3228–3234. <https://doi.org/10.1128/AEM.04018-14>.
- Guillier, L., Augustin, J.C., 2006. Modelling the individual cell lag time distributions of *Listeria monocytogenes* as a function of the physiological state and the growth conditions. *Int. J. Food Microbiol.* 111, 241–251. <https://doi.org/10.1016/j.ijfoodmicro.2006.05.011>.
- Koutsoumanis, K., 2008. A study on the variability in the growth limits of individual cells and its effect on the behaviour of microbial populations. *Int. J. Food Microbiol.* 128 (1), 116–121. <https://doi.org/10.1016/j.ijfoodmicro.2008.07.013>.
- Métris, A., George, S.M., Baranyi, J., 2006. Use of optical density detection times to assess the effect of acetic acid on single-cell kinetics. *Appl. Environ. Microbiol.* 72 (10), 6674–6679. <https://doi.org/10.1128/AEM.00914-06>.